NTNU
Norwegian University of Science and Technology

Automatic Equalization of Ship Noise Measurements

Yajing Wang

June 25, 2019

Abstract

The geometric spreading correction for noise level measurement is not so accurate since the noise also affected by the surface and bottom reflection. The surface reflection interference is called Lloyd mirror effect. A model to reduce the Lloyd mirror effect was designed. Thereby more accurate noise spectrum of ships can be obtained, the origins of the noise generator can be found. Further more increasing the catch rate.

The experiment was conducted on Gunnerus(a research vessel belong to NTNU) in Trondheim fjord, September, 2018. The hydrophone located close to the sea bottom and the vessel following straight tracks of 1 km and passing the hydrophone. The result of the experiment confirmed that the Lloyd mirror effect interfered the measured noise level. By using the inverse model, the Lloyd mirror effect was reduced in some extent.

Acknowledgements

his thesis is carried out by Yajing Wang as a part of the Master of Technology study at Norwegian University of Science and Technology (NTNU). The work was carried out during the the autumn semester of 2018 and spring semester of 2018 under supervision of Professor C and Professor Jens Hovem. I would like to thank Hefeng Dong and Jesn Hovem for giving me invaluable inputs regarding the project and report during our meetings throughout the semester.

ii

Contents

List of Figures

Chapter 1

Introduction

The motivation of this thesis is that self-noise generated from fishing vessels may effect the catch rate. The commercial fish hearing threshold tells us the frequency range and intensity of the sound that fish can sense, comparing this threshold with the noise spectrum of the fishing vessel will help us to find if the noise generated by the ship can be sensed by fish or not. Furthermore to find the origins of the noise(which can be sensed by fish): whether the noise is coming from the propeller cavitation or from vibration in the hull. Then maybe we can find a way to reduce the intensity of the noise that generated from the particular part of the ship. To achieve this goal a accurate method to correct the measured t noise level is needed. The old method is to correct the measured noise level with the geometric spreading which is $20log(r)$. It didn't take the Lloyd mirror effect into consideration, the Lloyd mirror interference effect distorted the noise which gives a not correct noise level. So the final goal of this thesis is to design a model to compensate the Lloyd mirror effect.

1.1   Thesis Outline

This thesis will be organized as follows.

Chapter 2 - Theory: Background theory needed for this thesis is covered.

Chapter 3 - Method: The implementation of the experiment.

Chapter 4 - Results and Discussion: The simple inverse model is presented.

Chapter 5 - Conclusion: Concluding remarks.

Chapter 2

Theory Part 1

This chapter will cover with some of the background theory needed for this thesis. The subsequent sections will give the basic knowledge of sound, Transmission loss equation with geometric spreading. The classified types of underwater noise, the commercial ships noise and fish hearing threshold will be presented. The octave band will be explained. After that the Lloyd mirror effect will be explained Finally the method of cancelling the Lloyd mirror effect will be presented.

2.1 Sound

Sound is a disturbance propagated through an elastic medium causing a detectable alteration in pressure or a displacement of the particles.
Sound is transmitted as waves, there are several properties can be used to characterized the sound wave. These properties are listen below:

- Frequency: frequency is measured as the number of wave cycles that occur in one second. The unit of the frequency is Hertz (Hz).

- Amplitude: the loudness of the sound correspond to the amplitude of the wave.

- Speed of sound: it is depends on many factors, such as: volume stiffness, or bulk modulus, and the density of the medium. In underwater acoustics,

also depend on water temperature, salinity, and the surrounding pressure or the depth of the water. A simplified formula after Del Grosso (1974) is:

$$c = 1448.6 + 4.618T - 0.0523T^2 + 1.23(S - 35) + 0.017D \qquad (2.1)$$

where c is the sound speed, T is the temperature, S is the salinity, D is the water depth. The speed of sound in air is around 343 m/s, in water it is around 1500 m/s.

Sound can be measured as pressure or intensity, sound pressure is the force of sound on a surface area perpendicular to the direction of sound, the SI-units for the sound pressure are N/m^2 or Pa. Sound pressure is often measured as a level on a logarithmic decibel scale. The sound pressure level (SPL) is defined as

$$SPL = 10 \log_{10} \frac{p^2}{p_{ref}^2} = 20 \log_{10} \frac{p}{p_{ref}} \quad \text{dB} \qquad (2.2)$$

where p is the root-mean-square sound pressure and p_{ref} is a reference sound pressure. In marine aquatics this reference pressure is 1 μPa.

Sound intensity is defined as the power carried by sound wave per unit area in a direction perpendicular to that area, the SI-unit fro the sound intensity is W/m^2. Sound intensity level is the level of the intensity of a sound relative to a reference value.

$$L_I = 10 \log_{10} \frac{I}{I_0} \quad \text{dB} \qquad (2.3)$$

where I is the sound intensity, I_0 is the reference sound intensity.
The sound intensity is proportional to the pressure squared:

$$I \propto p^2 \qquad (2.4)$$

2.2   Transmission Loss

In underwater acoustics there are two simple approximations were used to describe a sound wave propagates away from a source: spherical spreading and cylindrical spreading.

Spherical spreading describes the decrease in level when a sound wave propagates away from a source uniformly in all directions. Cylindrical spreading describes

in a medium with upper and lower boundaries can be obtained by assuming that the sound is distributed uniformly of a cylinder having a radius equal to the range r and height H equal to the depth of the ocean. During the spreading the sound intensity will decrease, the amount by which intensity decreases relative to its level at source is called transmission loss. The transmission loss is proportional to $1/r^2$ in spherical spreading, and $1/r$ in cylindrical spreading, this is based to their geometries.

In reality, the transmission loss depends on many factors - local bathymetry, the sound speed along the propagation, oceanographic conditions, and attenuation (a function of frequency). If encountered with the interaction with the sea surface and sea bottom reflections the situation will be much more complicated. Here we will apply very simple transmission model which depend only on geometric spreading (spherical sound propagation) and absorption, defined as

$$TL = 20log(r/r_0) + (r - r_0)\alpha_{dB} \qquad (2.5)$$

where α_{dB} is the absorption coefficient in dB per meter, r is the distance between the transmitter and the receiver, r_0 is the reference distance that is usually selected to be $1\,\mathrm{m}$. When r_0 is much smaller than r, the equation above becomes

$$TL = 20log(r) + r\alpha_{dB} \qquad (2.6)$$

Figure 2.1 shows a plot of equation 2.6 which gives a intuitive cognition of transmission loss in different frequencies versus the range. $\alpha = 0.05 f_{kHz}^{1.4}\mathrm{dB/km}$ is used in Figure 2.1.

In section 2.8 discussed the propagation involves the interaction with the sea surface (only one time reflection), it has a significant impact on transmission loss, actually the sea bottom reflection also play a important role here but this is not our interests in this context.

2.3   Underwater Noise

2.3.1   Underwater Ambient Sound

Ambient noise is contributed from many sources, both natural and anthropogenic. These sounds combine to give the continuum of noise which interferes all the
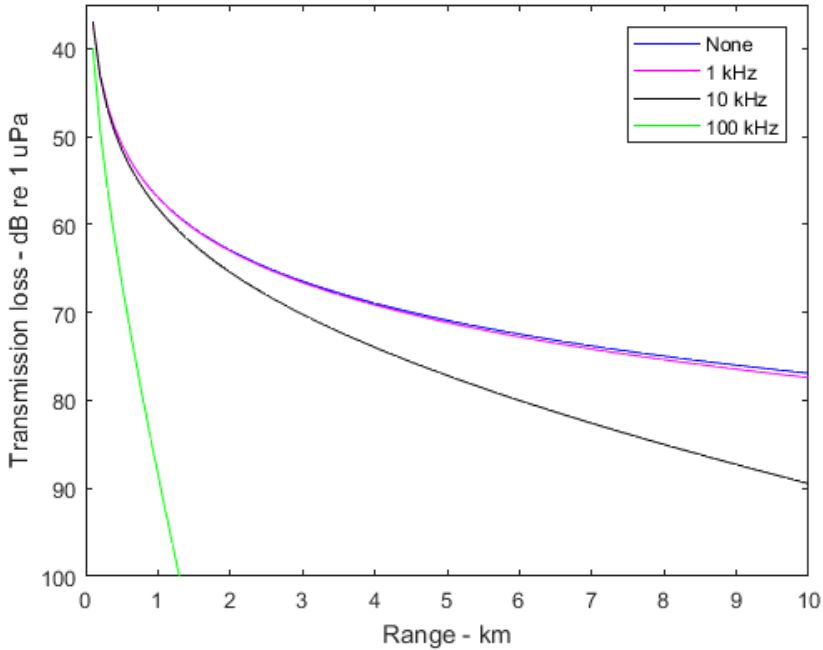
Figure 2.1: The transmission loss verses range in different frequencies (this transmission loss as defined in equation 2.6 with $\alpha = 0.05 f_{kHz}^{1.4} \mathrm{dB/km}$
)

signals propagating underwater. The frequency range of underwater ambient noise is from 1 Hz to 100 kHz. Urick (Urick 1983) classified sources of ambient noise in the ocean into six categories:

- From tides and hydrostatic pressure change of relatively large amplitudes and at low-frequency.

- Seismic disturbances that generates noise between 1 and 100 Hz.

- Ocean turbulence in the form of irregular random water currents of large or small scales (Wens 1962),For instance, steady current at 1 knit can generate noise around 106 dB (re 1 μPa).

- Ship traffic that generates frequency in the range of 50 to 500 Hz-Such noise can be detected at distances of 1000 miles or more.

- Surface waves that caused noise in the frequencies between 1 and 50 kHz (NRC 2003)-When below 5 to 10 Hz, the dominant ambient noise source was the nonlinear interaction of oppositely propagating ocean surface waves.

- Noise caused by precipitation (rain, hail, snow). The spectrum of rain noise, for wind speeds below 1.5 m/s, showed a peak at 13.5 kHz with a sharp cutoff on the low-frequency side.

2.3.2 General Ship Noise

Growth pf the global shipping fleet and possibly the average size of ships has raised deep-ocean noise level. Figure 2.2 shows the source levels for various classes of ships which can give us a basic cognition about noise generated from ships.
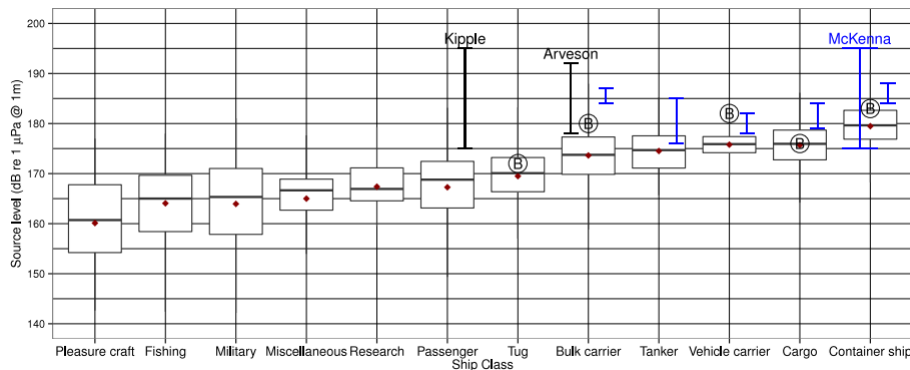
Figure 2.2: Comparison of source levels form different studies for various class of ships (Adapted from "Ship noise extends to frequencies used for echolocation by endangered killer whalesScott" by Veirs , Val Veirs and Jason D. Wood, 2016, *The Journal of Life and Environmental Sciences*, page 6, Copyright 2016 Veirs et al.)

Commercial Ship Noise

Commercial ship noise is generated primarily from propellers cavitation, propeller singing, engine and on-board machinery and hull form. The most of the underwater noise is caused by propeller cavitation which has peak power near 50-150 Hz.

Cavitation is the formation and dissolution of vapor-filled voids (vapor bubbles) in liquid mediums. Propeller singing is caused by blades resonating which emits strong tones between 100 and 1000 Hz, and other machinery has peak power below 50 Hz. One type of ships need to be mention here is fishing vessels. Fishing vessels are boats and ships designed to catch fish and marine wildlife. A bottom trawl is a towed fishing gear that is designed to catch fish, shrimp, or other target species live on or in close to the seafloor. Trawling operation produced noise tones is from 10 to 10 000 Hz.

2.4   Fish Hearing

For many species of fish, the low-frequency sounds which were mentioned in section 2.3.2 occur directly within their hearing range. Figure 2.3 shows the relationship that exists between commercially harvested species hearing threshold and sound frequency.
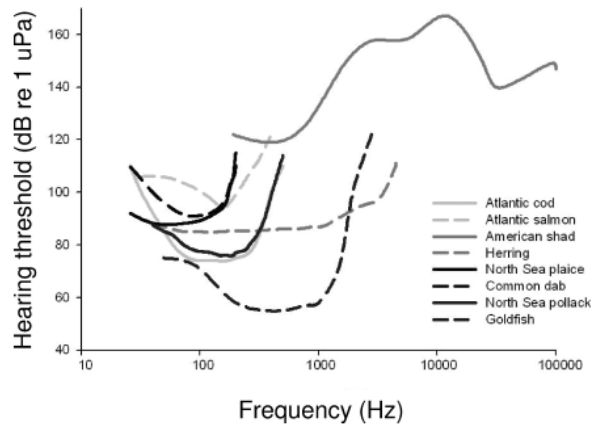
Figure 2.3: Audiograms of fish hearing sensitivity for several commercial species (Adapted from *Behavior of Marine Fishes: Capture Processes and Conservation Challenges*, by Paul D. Winger Steve Eayrs Christopher W. Glass, 2010, Copyright 2010 Blackwell Publishing Ltd

2.5 Octave Bands Analysis

Octave bands are used when the frequency composition of a sound is needed to be determined. Octave analysis is often used in noise control. An octave band is the upper band frequency f_u is twice the lower band frequency f_l, the mathematical form is

$$f_u = 2f_l \tag{2.7}$$

The center frequency of an octave band is

$$f_c = \sqrt{f_u f_l} \tag{2.8}$$

The 1/3 and 1/24 octave bands are often used. 1/3 octave is equal to one third of an octave and 1/24 is equal to one 24th of an octave. In other words they presents a more detailed analysis than octave bands. Then the relation between the upper frequency and lower frequency with concern of 1/3 and 1/24 is

$$f_l = \sqrt[Q]{2} f_u \tag{2.9}$$

where Q is the octave bandwidth specified by the Bandwidth property. For example, if Bandwidth is specified as '1/3 octave' ,then the Q is 3.

2.6 Multi-path Propagation

Multipath is formed by two effects: sound reflection and sound refraction. Figure (2.4) shows how reflections forms multipath.
Actually there are much more paths than these paths indicated in the figure due to refraction and multiple reflections, but most of them can be negligible since that they have undergone multiple reflections and lost much of the energy. The significant paths here are the first order surface reflected and bottom reflected waves which still contains non negligible energy to interfere the direct wave.

In order to distinguish the direct path and the first order reflected path, the first thing we need to know is if the wave is reflected by the sea surface or bottom. The reflection coefficient can tell the character of the reflected wave, which is expressed by:

$$R_\phi = \frac{\Phi_r}{\Phi_i} = \frac{\rho_2 c_2 \sin\theta_1 - \rho_1 c_1 \sin\theta_2}{\rho_2 c_2 \sin\theta_1 + \rho_1 c_1 \sin\theta_2} \tag{2.10}$$
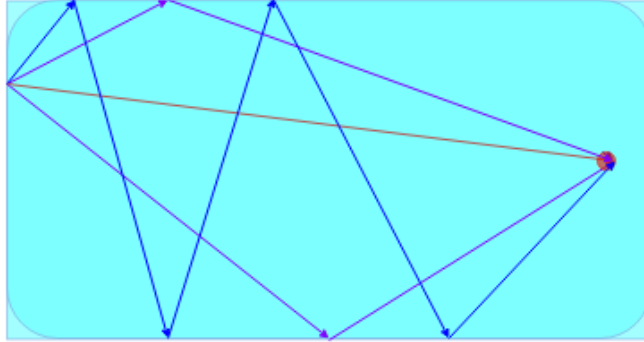
Figure 2.4: Sketch of the multipath ($SourceDepth = 6m, ReceiverDepth = 20m$, The orange line presents the direct arrival, the two purple line presents the first order reflection, the blue line presents a multi times reflection)

Where the Φ_r is the amplitude of the reflected wave, Φ_i is the amplitude of the incident wave. ρ_1 and ρ_2 are densities of the incident media and transmission media, c_1 and c_2 are the sound speed of the incident media and transmission media, $\sin\theta_1$ and $\sin\theta_2$ are the incident angle and reflected angle. Equation (2.10) gives the information about how the phase shifts and amplitude changes of the reflected wave compare to the incident wave, furthermore it can be used to analyze the received signal.

2.7   Bellhop Ray Tracing Method

Bellhop is a highly efficient ray tracing program to model the multipath propagation conditions. It is designed in order to perform two-dimensional acoustic ray tracing for a given sound speed profile and ocean channel boundaries conditions. Bellhop is theoretical based on the ray acoustics, where ray acoustics is based on the assumption that the sound propagates along rays that are normal to wave fronts. When the sound speed is constant the ray follows straight line paths, but in the sea water the sound speed is not constant the ray then follows curved paths, and the ray bends towards the region of lower propagation speed. In general Bellhop calculates the direction of the rays by using the sound speed profile. When the ray encounter the boundaries of the ocean channel the BELL-HOP will calculate the energy loss and polarity of the rays with the help of the reflection coefficient and absorption coefficient. The result given by BELLHOP

can be used to check the characteristics of the channel.

2.8 Lloyd's Mirror Effect

The ocean acoustic Lloyd's Mirror Effect is a special case of the multiple path propagation presented in Section 2.6. Lloyd's Mirror Effect only contain interference effects produced by the direct and surface-reflected acoustic paths. See Figure 2.5 for figurative illustration. The reflected wave can be considered sent
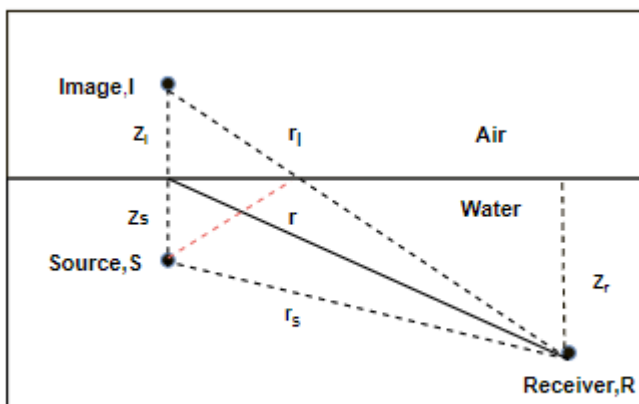
Figure 2.5: The Lloyd's Mirror geometry (r_S is the direct path from the source S, r_I is the modeled reflected path, the distances to the Source and Image source are equal ($Z_S = Z_I$)

by the image source I. Lloyd's mirror interference effect can be understood by the superposition of a source with strength, ρ_{os}, and its image source strength multiplied by the reflection coefficient R,$R\rho_{os}$. Since the pressure is additive, the received pressure at R is the sum of the radiated pressure from the source and its image:

$$P[r,t] = P_s[r_s,t] + P_i[r_i,t] \qquad (2.11)$$

The radial distance from the source and its image source can be determined
directly from the geometry:

$$r_{s,i} = [r_h^2 + (z_r \mp z_{s,i})^2]^{1/2} \tag{2.12}$$

where r_h is the horizontal distance between the receiver and source. Now assumes
the source is simple harmonic, and the interface is considered a smooth surface
with reflection coefficient $R = -1$, the sound pressure at receiver can be written
as:

$$P[r,t] = \rho_{os}\frac{e^{ikr_s}}{r_S} - \rho_{os}\frac{e^{ikr_i}}{r_i} \tag{2.13}$$

Knowing the pressure we can calculate the intensity with:

$$I = (1/2\rho c)\text{Re(pp*)} \tag{2.14}$$

Combining the two equations (2.13) and (2.14), we obtain the intensity at the
receiver:

$$I = I_{os}[1/r^2]2[1 - cos(2kz_r z_s/r)] \tag{2.15}$$

The cosine in the equation above determines the maxima and minima in the in-
tensity

The transmission loss level which taking the Lloyd mirror effect into consideration
can be calculated by:

$$TL = 10log(I/I_{os}) = 10log[1/r^2] \cdot 2 \cdot [1 - cos(2kz_r z_s/r)] \tag{2.16}$$

Figure2.6 shows the relative transmission loss level in different frequencies versus
range. Figure 2.6 illustrates the Lloyd mirror effect interfere the sound intensity
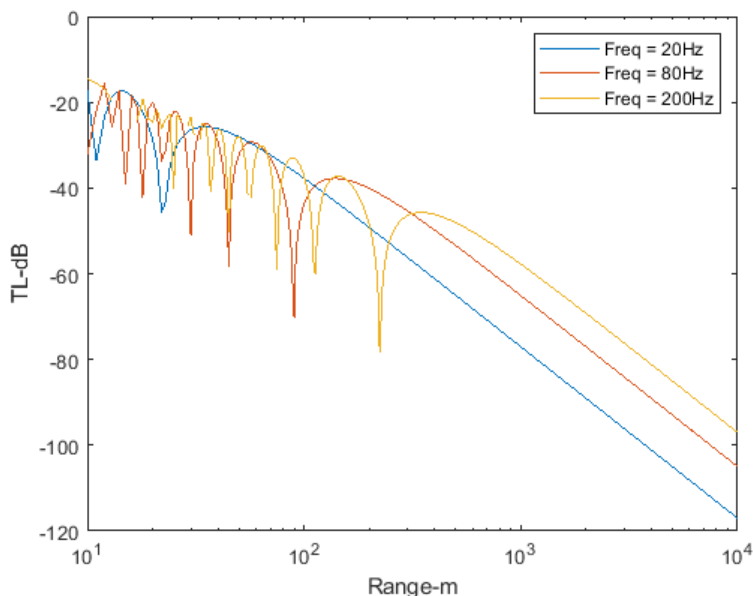in near field, in the far field the sound intensity decreases as $40log(r)$.

Figure 2.6: Transmission loss from a source at 6 m depth to a receiver at 140 m depth as a function of range and frequency

2.9 A Simple Inverse Filter

An underwater channel is dynamic, the impulse response of the underwater channel then describes the changes of it. Generally we excite the channel with a impulse signal $\delta(t)$, the received signal is the impulse response of the channel at that moment. The signal used to get the channel impulse response will be described in section 2.9.1. The primarily problem of this impulse response is the Llyod's mirror effect, the direct path and the first order reflection path arrive at the receiver almost simultaneously, the impulse response at that moment is overlapped and distorted. A commonly used method to distinguish the direct arrival and first order reflected arrival is called matched filter, this technique will be well explained in section 2.9.2. With the information of the channel impulse response a simple inverse filter can be built to cancel the Lloyd's mirror effect from the signal, the section 2.9.3 will describe a simple method about how to make a inverse filter. .

2.9.1   The Chirp Signal

Normally we will excite the system with a **Dirac delta function($\delta(t)$)** and the received signal $y(t)$ is the impulse response of this channel. However the good performance of underwater channel detection depends on the transmitted signal energy, and the signal's amplitude is constrained by a power limitation in the transducer. The solution is to increase the length of transmitted signal, so $\delta(t)$ is not a option here. The solution is the linear chirp signal where the frequency sweeps across a frequency band B during time T. The chirp signal can be expressed by the equation

$$p(t) = p_0 \cos[2\pi(f_0 t + \frac{1}{2}mt^2)] \tag{2.17}$$

$$-T/2 < t < T/2 \tag{2.18}$$

where m is the rate of frequency change, f_0 is the carrier frequency(center frequency). The instantaneous frequency f_t varies exactly linearly with the time:

$$f_t = f_0 + mt \tag{2.19}$$

which varies from $f_0 - \frac{mT}{2}$ to $f_0 + \frac{mT}{2}$. Therefore the bandwidth is approximately $B = mT$ and consequently

$$m = \frac{B}{T} \tag{2.20}$$

Equations above defines an up-slope chirp signal where the frequency increases linearly with time. To detect the Lloyd Mirror effect the time resolution of the chirp signal should be shorter than the time difference between the direct and reflected arrival.

2.9.2   Matched filter technique

Match filter is a signal processing technique commonly used by sonar to increase the range resolution as well as the signal to noise ratio. This is achieved by modulating the transmitted pulse and them correlating received signal with the transmitted pulse.

The received signal, written $r(t)$, is an attenuated and time delayed copy of the original transmitted signal. There is also noise in the received signal which we

use $B(t)$ to denote the the noise. Another thing needed to mention here is when the source or/and receiver is not static, Doppler effect can play a role too, we write f_D to denote the Doppler shift.

The cross correlation of the received signal with the transmitted signal is computed by convolving the received signal with a conjugated and time-reversed version of the transmitted signal. Which is:

$$w(\tau) = \int_0^T s^*(t')r(t-\tau)dt \qquad (2.21)$$

where $s^*(t')$ is the conjugated time-reversed transmitted signal, T is the duration, and $r(t-\tau)$ is the received signal. The time τ is the time delay between the source waveform and any received echoes.
Now we add the Doppler effect into the equation (2.21), the absolute value of the cross correlation can be expressed as:

$$|w(t, f_D)| = \left| \int_0^T s^*(t')r(t-\tau)e^{2\pi i f_d t}dt \right| \qquad (2.22)$$

The equation (2.22) represents the cross correlation with a frequency shift f_D. Since we already chosen the chirp signal as the transmitted signal, due to the property of the chirp signal the Doppler effect can be replaced with a frequency shift f_D of the carrier frequency. Inserting the chirp signal to equation (2.22), we obtain:

$$|w(t, f_D)| = |(1 - \frac{|\tau|}{t})\frac{sin[\pi(B\frac{\tau}{T} - f_D)(T - |\tau|)]}{\pi(B\frac{\tau}{T} - f_D)(T - |\tau|)}| \qquad (2.23)$$

Where B is the bandwidth for the chirp signal, equation 2.23 presents the compensated channel impulse response.

2.9.3 Inverse Filter

The idea behind inverse filtering is to form a computational model for the channel and then to cancel its effect from the signal by filtering the signal through the inverse of the model. In other words the Inverse filters are used to reducing the unwanted channel effects of the signals, the unwanted effect here is the Lloyd's mirror effect.
Since in the frequency domain the received signal $R(\omega)$ is:

$$R(\omega) = S(\omega)H(\omega) \qquad (2.24)$$

Where $S(\omega)$ is the source signal in the frequency domain and $H(\omega)$ is the channel impulse response in the frequency domain. Then the direct approach to compute the inverse filter is inverse the $H(\omega)$ which is $H^{-1}(\omega) = 1/H(\omega)$, the problem here is there are many zeros in the transfer function $H(\omega)$ which resulting in dividing by zero.

A simple channel model can avoid the zero error here, it assumes that the channel is two delta functions separated in time. Figure 2.7 depicted this simple model. The first delta modeled the direct path with amplitude A_1. the second delta
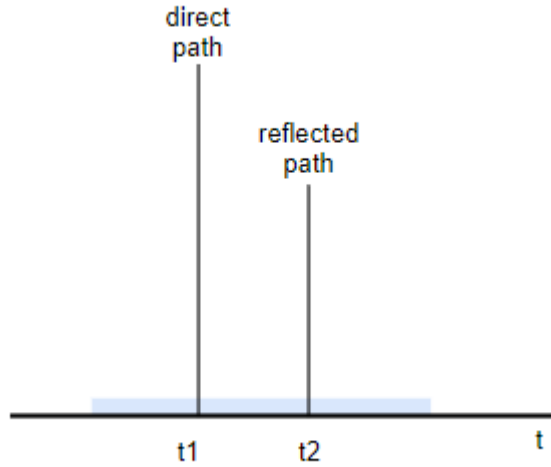

Figure 2.7: The modeled impulse response

modeled the surface reflected path with amplitude A_2, the time duration ($\tau = t2 - t1$) between them is the time differences between the direct and reflected arrival. The transfer function $H(\omega)$ turned to:

$$H_\omega = A_1 - A_2 e^{j\omega\tau} \tag{2.25}$$

The minus sign before A_2 is because the reflection coefficient is negative when it is surface reflected.

The inverse transfer function is:

$$H^{-1}(\omega) = \frac{1}{A_1 - A_2 e^{j\omega\tau}} \tag{2.26}$$

This division form is not perfect when encountered very low frequency and the condition $A_1 \approx A_2$, since the low frequency will lead the term $e^{j\omega\tau}$ closes to 1, the

approximately equal amplitudes will lead the term $A_1 - A_2$ approaching to zero, the inverse transfer function approaches infinity while denominator approaching to zero, then this inverse transfer function fails. However the form of this equation reminds us the Taylor series

$$\frac{1}{1-x} = \sum_{n=0}^{\inf} x^n, for -1 < x < 1 \tag{2.27}$$

So the equation 2.26 can be expanded as:

$$H^{-1}(\omega) = 1 + \frac{A_1}{A_2}e^{j\omega\tau} + \frac{A_1}{A_2}e^{2j\omega\tau} + \frac{A_1}{A_2}e^{3j\omega\tau} + ... \tag{2.28}$$

A_2 should be always smaller than A_1 since the ocean surface is not mirror flat, there will be energy loss in reflection. Then the term $\frac{A_1}{A_2} < 1$. The time duration between the direct arrival and reflected arrival will be only several milliseconds, therefore the term $e^{j\omega\tau}$ will be smaller than 1 too. There is no worry that the whole part $\frac{A_1}{A_2}e^{j\omega\tau}$ will over the limit. Finally equation 2.28 is the simple inverse filter.

Chapter 3

Method

[RO, LE]Chapter 3: Method

3.1   Signal generation

A LFM signal was generated to estimate the channel impulse response. The parameters of the signal see Table 3.1

Sampling Freq	Bandwidth(Hz)	Center Frequency	Time one LFM(s)	Silence Time(s)
44100	7000-17000	12000	1	9

This bandwidth and time duration of the LFM was designed followed the time resolution rules in section 2.9.1.

3.2   The Experiment

This experiment was conducted in Trondheim fjord on September, 2018 using Gunnerus(a research vessel belong to NTNU). Figure (3.1) depicts the basic in-
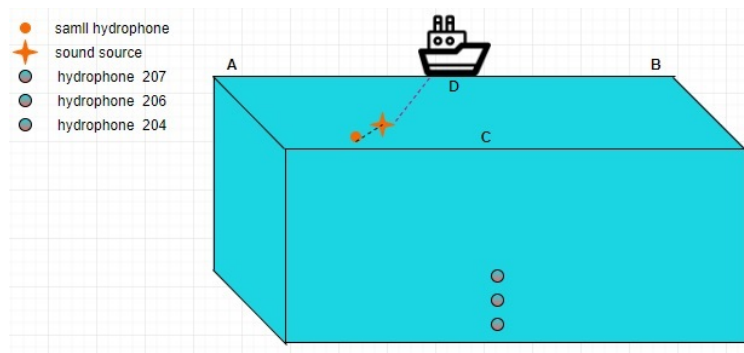
formation about the vessel route.

Figure 3.1: The hydrophones positions and vessel route

Table 3.1 states the locations of position A, position B, position C, three hydrophones.

Locations	Distance
A [Water Depth]	150 m
B [Water Depth]	150 m
c [Water Depth]	130 m
A-B	1040 m
A-C	520 m
B-C	530 m
C-D	30 m
A-204, 206, 207	535 m , 533.8 m, 532.7 m
B-204, 206, 207	544.7 m, 543.5 m, 542.4 m
C-204, 206, 207	134 m, 130 m, 125 m

Three hydrophones were used to measure the chirp signal and noise generated by the vessel, one thing need to mention here is none of them were placed to the expected positions, the perfect position for the hydrophones is really close to the sea bottom, in other words they should be placed exactly on the bottom.

The CTD (Conductivity, Temperature, Depth) profiles were measured at position C. Then the vessel navigated one back and forth between A and B at a speed of approximately 2 knots (1.08 m/s) while towing a source transmitting the LFM signal (See 3.1). The whole route took 38 minutes.

3.3   Data analysis

MATLAB was the program used to processing the data.
The data recorded by Hydrophone 204 were used since it is closest to the sea bottom, it was less interfered by the sea bottom reflections.

3.4   BELLHOP Ray Tracing

The CTD profiles was used to calculate the sound speed from sea surface to bottom at position C. With inserted the sound speed and the geometric information in Table 3.2 in the program BELLHOP, the rays pattern from position D to the receiver and the time of arrivals were modelled.

3.5   Design of The Simple Model

Two special time sections were picked to do the processing. The first section was started at 60 s and ended at 70 s, which contained one chirp which is 1 s and 9 s noise. At the beginning of this time section the vessel located almost at the furthest place to the hydrophone. The second section was started at 360 s and ended at 370 s, which also contained one chirp which is 1 s and 9 s noise. During this time section the vessel passed through the nearest place to the hydrophone.

The raw data were plotted from the two sections both in time and frequency domain. Then the matched filter 2.23 were applied to both sections, the data were plotted. After that the amplitudes of the first arrival and surface reflected were found, also the time duration between the two arrivals was found. The simple channel impulse were calculated by the equation 2.25. Next the inverse filters for these two time sections were calculated by equation 2.28.

A three seconds noise was picked from each time section, plotted in frequency domain. Then both of them correlated with their inverse filters, the results were plotted.

3.6   Transmission Loss

A 3 s time section of noise was picked every 54 s from the first half of the recorded signal, this was corresponding to every 60 m on the route A-B. All of them were transformed to frequency domain, then the noise levels for frequency 20 Hz and frequency 80 Hz were found in all the 18 sections and plotted.

Chapter 4

Results And Discussion

This chapter will present the result of the simple inverse channel model. All the processing results are obtained from Matlab. The subsequent sections will show the steps needed to design the inverse model. After that the measured transmission loss for the whole route will be presented. Lastly the time difference trend of the direct arrival and surface reflected arrival will be shown.

4.1 Raw data

The raw data extracted from the receiver (Hydrophone 204) from $113\,\mathrm{s}$ to $173\,\mathrm{s}$, there are six pile of overlapping pulses in a chaotic jumble. Actually this is the impulse response of channel, but it contained too much information(bottom reflection due to the hydrophone was not on the sea floor, ambient noise, other ships noise ...) that we don't need here. The information we need is: the relatively amplitudes of the direct and surface reflected arrivals, the time differences between the two arrivals.
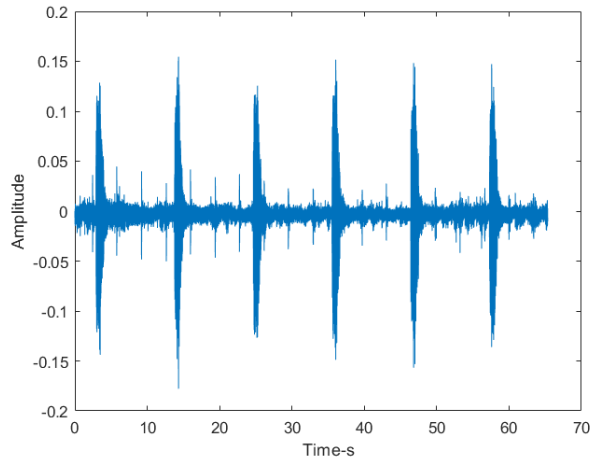
Figure 4.1: The data directly read from the Hydrophone 204

4.2   The Channel Impulse Response

The left plotting in Figure 4.2 shows the raw data marked as *data 1* (started at 60 s ended at 70 s). The right plotting in Figure 4.2 shows the same data in the frequency domain. The Overlapping pattern in (a) in Figure 4.2 is the
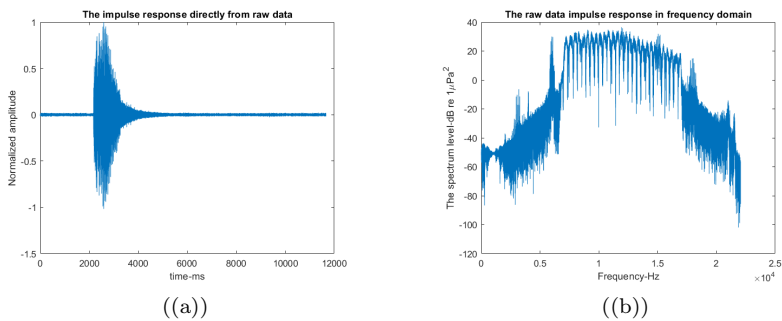

((a))

((b))

Figure 4.2: The raw data

interference effect from multiple surface and bottom reflections.
The matched filter was applied to this data, the result shows in Figure 4.3, the

amplitudes were normalized. The right plotting in Figure4.3 is the amplified version of the left one, there are two pulses with a time difference of $3\,\text{ms}$. This result matched our expectation since the sound source is approximately $500\,\text{m}$ to the hydrophone.
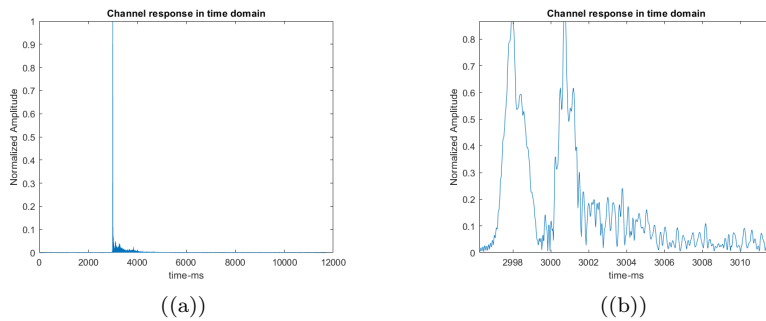

((a))   ((b))

Figure 4.3: The impulse response in time domain

Figure 4.4 shows Bellhop modeling result of the signal section(marked as *data 2*) from 360 s to 370 s. Figure (a) shows the sound speed profile at position C and the six Eigen rays reached the receiver, two direct arrival, two surface reflection arrival and two seabed reflection arrival. There were more rays modeled by the Bellhop, they only contained a little energy, therefore they were ignored here. Figure (b) shows the amplitudes, arrival time, polarities of the first four rays. The polarity of the second arrival is negative so it was reflected from the sea surface, its amplitude is approximately 80% of first arrival(direct arrival). From the polarity and amplitude of the third arrival we know it was reflected from the seabed, also the energy is around one third of the direct arrival.
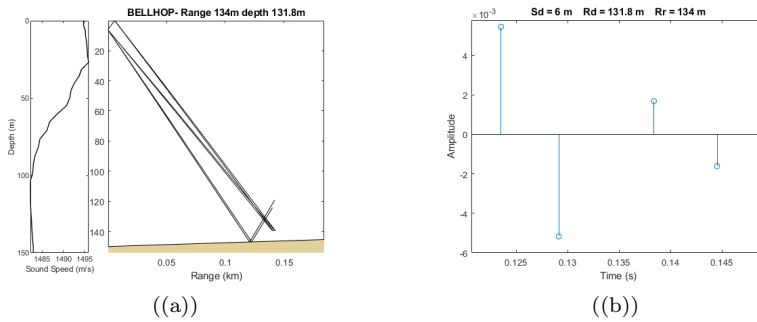
((a))   ((b))

Figure 4.4: BELLHOP model

Figure 4.5 shows the raw data section(from 360 s to 370 s) both in time and frequency domain. One thing should be notice here is the spectrum amplitude from 7000 Hz to 17 000 Hz is around 50 dB in Figure 4.5 (b), the spectrum amplitudes in Figure 4.2 (b) for the same frequency range is around 30 dB. When the data 1 was recorded the distance between the vessel and the receiver is around 500 m, this is almost the furthest distance to the receiver. When the data 2 was recorded the vessel was passing by the shortest distance to the receiver. Since the sound wave sent by the source was spherical spreading, the transmission loss proportional to $1/r^2$, The smallest r gives the minimal transmission loss, similarly the biggest r gives the maximum transmission loss.
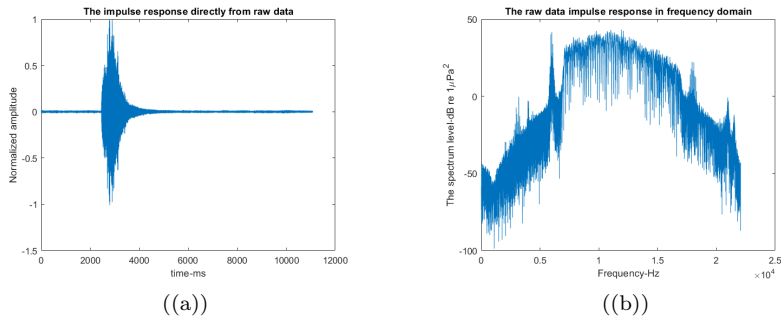
Figure 4.5: Raw data section 2

Figure 4.6 (a) shows the channel impulse response after applied matched filter technique. Figure 4.6 (b) shows the amplified version of the impulse response. The time difference is approximately 7 ms which is same as the BELLHOP modeled, see Figure 4.4. And also we can confirm this time difference from geometric calculation. The amplitude of the surface reflected arrival is around 60% of the direct arrival here is different from the BELLHOP modeled the surface reflected arrival is 80% of the direct arrival. It is obviously that the BELLHOP didn't take many factors into consideration such as: surface reflection loss, sea water absorption, wind, other noise source interference, objects in sea water... So the amplitude recorded is smaller than modeled.
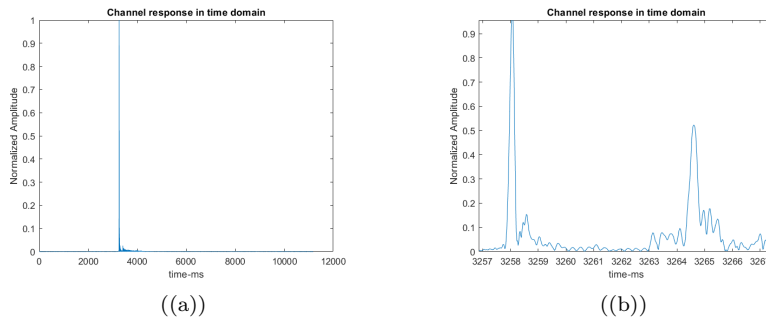

Figure 4.6: The impulse response in time domain

4.3   The Simple Channel Model

Figure 4.7 shows the simple channel response model of *data 1*, The values of the direct and surface reflected amplitudes, time difference between the two arrival were taken from Figure 4.3 (b). The curve presents the correction to transmission loss due to the Lloyd mirror interference effect in addition to geometric spreading loss. For low frequency range [10 Hz-200 Hz] the correction is -18 to $0\,\mathrm{dB}$, for higher frequencies the corrections oscillate significantly. This agrees with Figure 2.6 the low frequencies oscillates slowly and slightly while the higher frequencies oscillates significantly in near field.
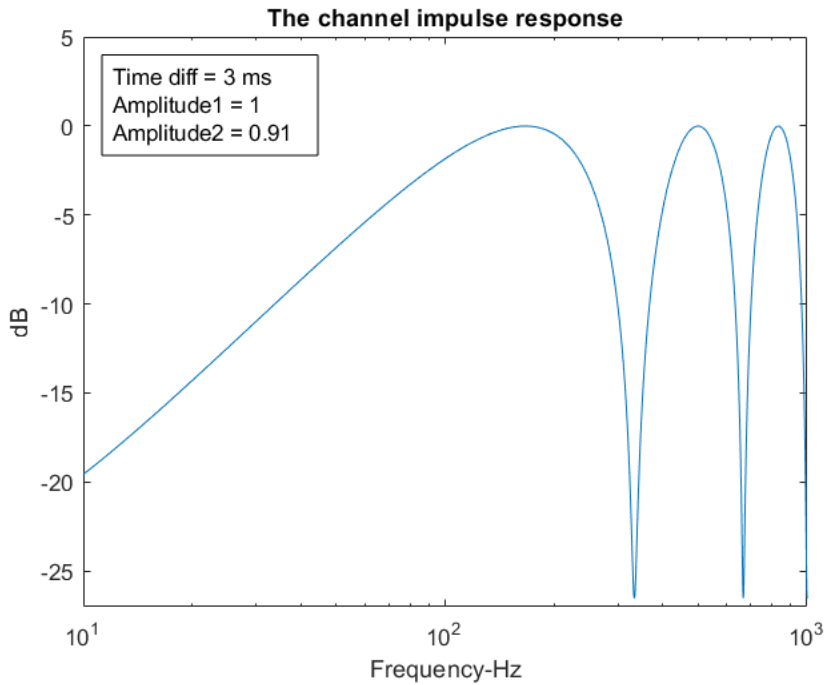

Figure 4.7: Simple channel impulse response model

Figure 4.8 shows the simple inverse channel model, the curve here is more in-
tuitive presents the correction to the transmission loss due to the Lloyd mirror
effect. This inverse filter illustrates that the transmission loss is approximately
25 dB for low frequency range [10 Hz-200 Hz] and this is almost same as the re-
sult presented in Figure 2.6. And for higher frequencies it compensated the Lloyd
mirror effect with significant oscillation.

Here is correction dB value is differ from the impulse response model and theo-
retically they should be same, one possible reason is the amplitudes of the direct
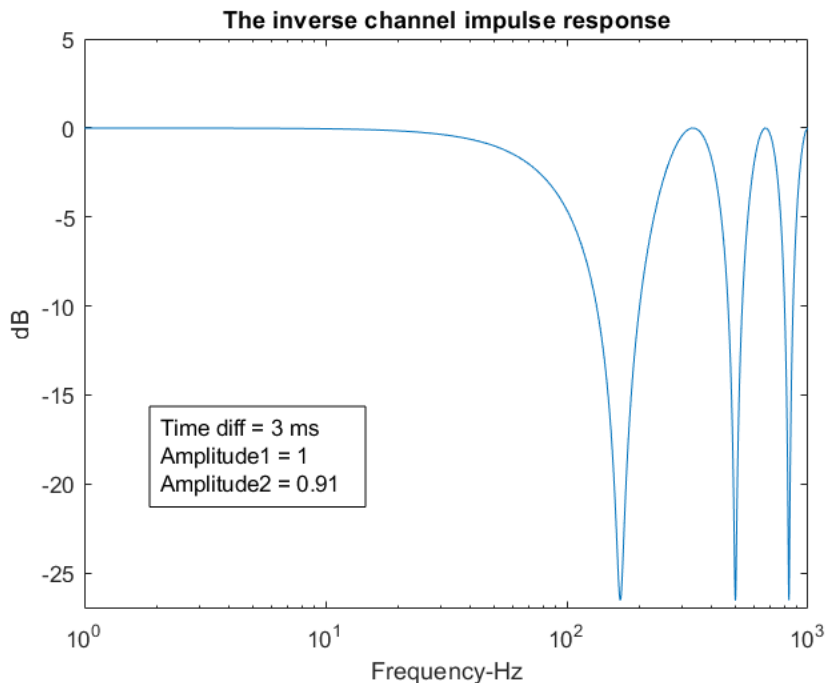arrival is almost same as the surface reflected arrival.

Figure 4.8: Simple inverse channel impulse response model

Figure 4.9 shows the simple channel response model of *data 2*, the values of the direct and surface reflected amplitudes, time difference between the two arrival were taken from Figure 4.6 (b). The curve presents the correction to transmission loss due to the Lloyd mirror interference effect in addition to geometric spreading loss. For low frequency range [10 Hz-200 Hz] the correction is -10 to $0\,\text{dB}$, for higher frequencies the corrections oscillate significantly. This agrees with Figure 2.6 the low frequencies oscillates slowly and slightly while the higher frequencies oscillates significantly in near field.
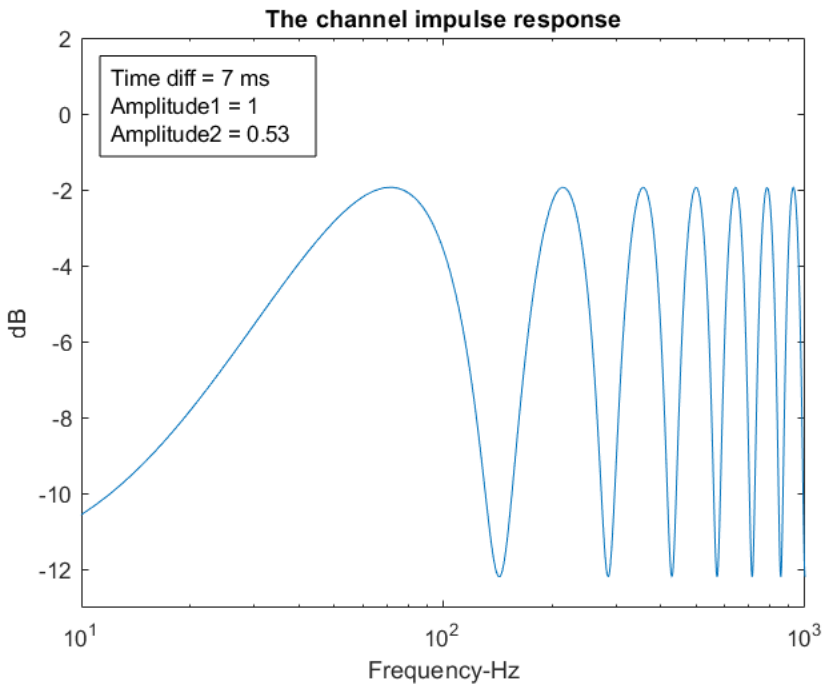

Figure 4.9: Simple channel impulse response model

Figure 4.10 shows the simple inverse channel model, same as the last inverse model the curve is more intuitively. The correction is -10 to $0\,\text{dB}$ fro low frequency range [10 Hz-200 Hz], This correction dB is same as the impulse response model and this is correct. For higher frequencies it compensates the Lloyd mirror effect with significant oscillation.
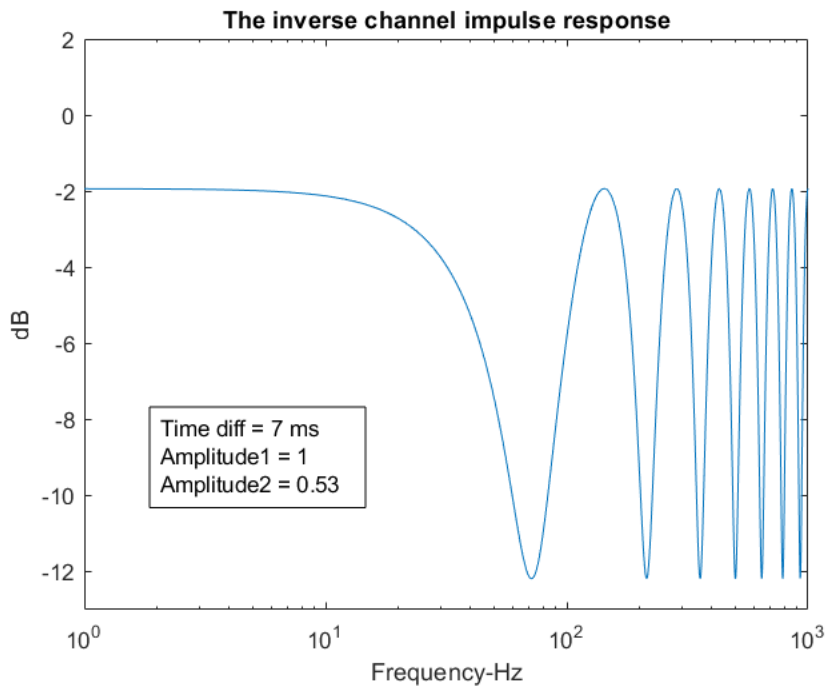

Figure 4.10: Simple inverse channel impulse response model

4.4   Noise Analysis

4.4.1   Noise Data 1

Figure 4.11 shows the noise spectrum, this data contains $3\,\mathrm{s}$ noise which was picked from *data 1*. This noise spectrum was overlapped, but we still can see there are one peak at $freq \approx 80\,\mathrm{Hz}$, another peak at $freq \approx 200\,\mathrm{Hz}$. The spectrum level decreases with the increases of frequency values. This trend illustrate that for same propagating range the higher frequency suffer more attenuation that lower frequencies.
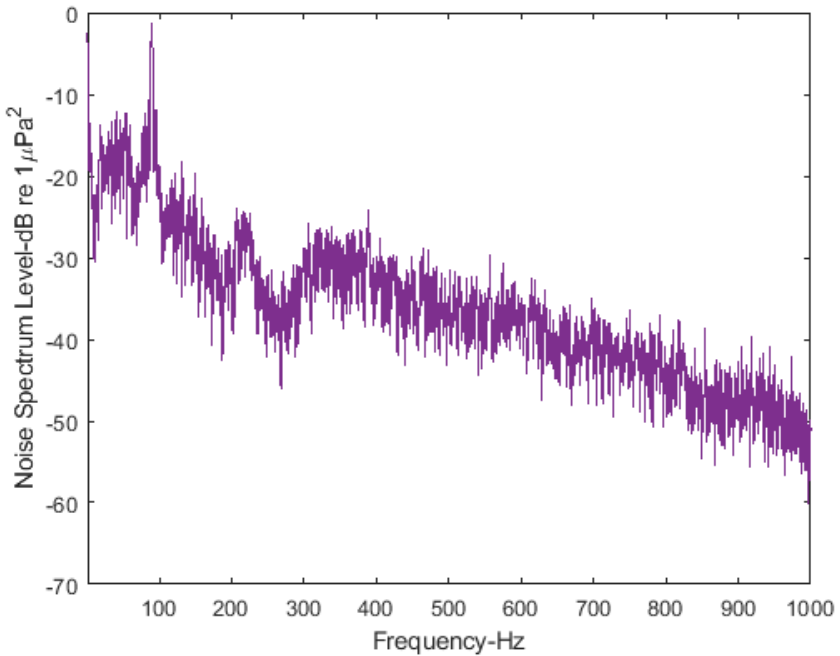

Figure 4.11: Noise Spectrum

Figure 4.12 shows the comparison of noise measured level in 1/24 octave bands and the Lloyd mirror effect corrected noise level 1/24 octave bands. The blue curve is the measured noise spectrum level, the purple curve is the corrected noise

level. Give a closer look to the frequency range [10 Hz-200 Hz] the purple curve is around 20 dB less than the blue curve this means the corrected noise level is is approximately 20 dB less than the measured level. In section 4.3 Figure 4.8 shows that a correction of −25 dB should be add to the transmission loss to correct the Lloyd mirror effect. So this inverse filter approximately achieved its purpose. This corrected noise curve oscillates irregularly may because the bottom reflection interference. Since the distance between the hydrophone and see bottom is around 5 m, the bottom reflected wave arrived just a few milliseconds later than the surface reflected arrival which can be seen in Figure 4.4 (b), this is the maximum time difference between the surface reflected arrival and bottom reflected arrival, it was only11 ms.
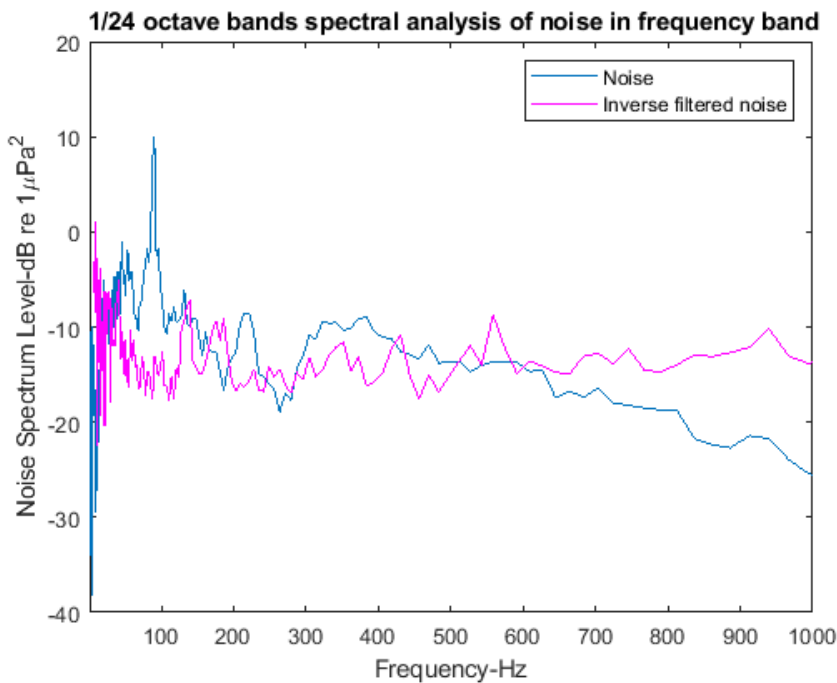

Figure 4.12: Noise spectrum in 1/24 octave bands

4.4.2   Noise Data 2

Figure 4.11 shows the noise spectrum, this data contains $3\,\mathrm{s}$ noise which was picked from *data 2*. We can see there is a peak at $Freq \approx 80\,\mathrm{Hz}$. The higher frequencies attenuated more than the lower frequencies.
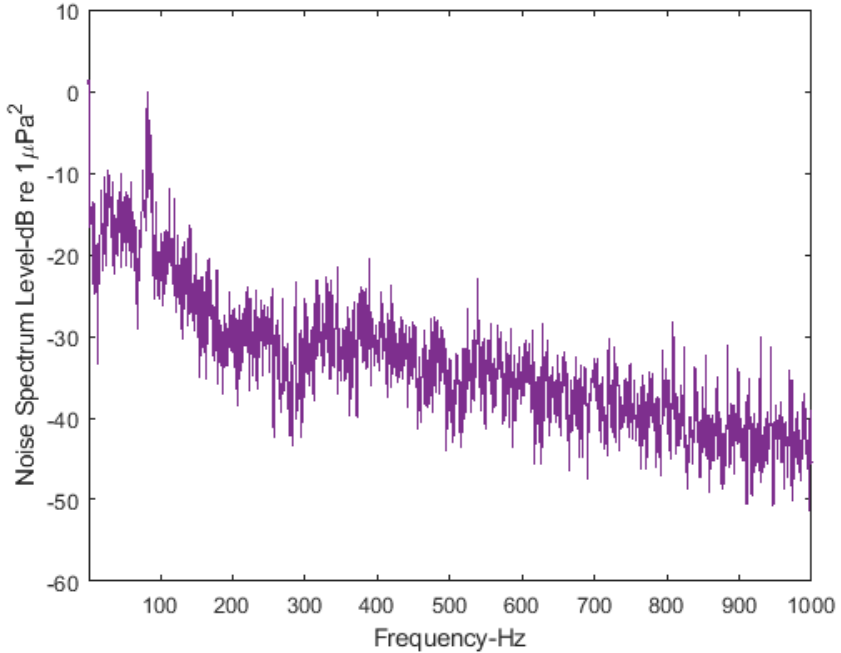

Figure 4.13: Noise spectrum

Figure 4.14 shows the comparison of noise measured level in 1/24 octave bands and the Lloyd mirror effect corrected noise level 1/24 octave bands. The blue curve is the measured noise spectrum level, the purple curve is the corrected noise level. Give a closer look to the frequency range $[10\,\mathrm{Hz}\text{-}200\,\mathrm{Hz}]$ the purple curve is around $10\,\mathrm{dB}$ less than the blue curve this means the corrected noise level is is approximately $10\,\mathrm{dB}$ less than the measured level. In section 4.3 Figure 4.10 shows that a correction of $-10\,\mathrm{dB}$ should be add to the transmission loss to correct the Lloyd mirror effect. So this inverse filter approximately achieved its purpose. It was also interfered by the bottom reflections, ambient noise, other

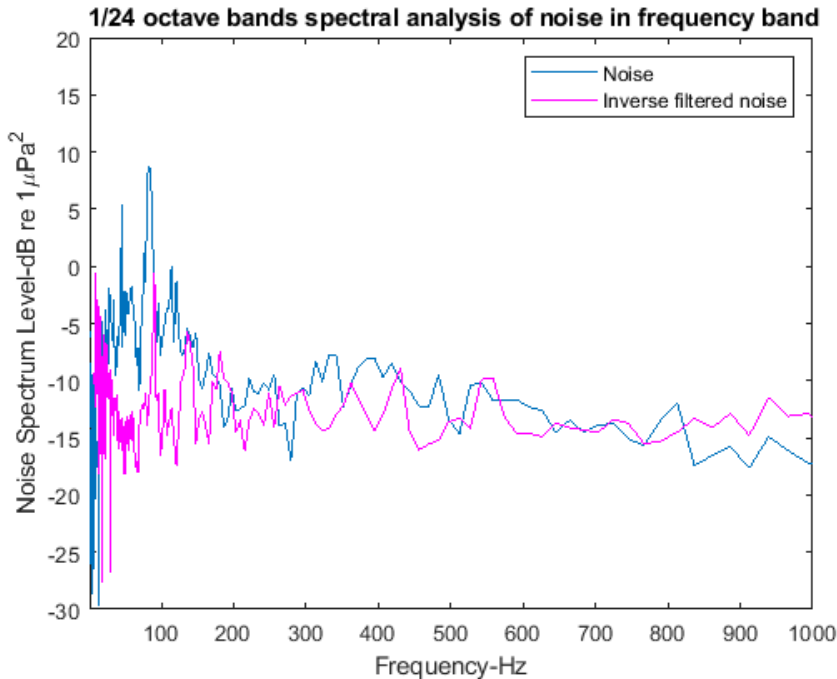ships noise, so the curve oscillates irregularly.

Figure 4.14: Noise spectrum in 1/24 octave bands

4.5 Transmission Loss And Fish Hearing

Figure 4.15 shows the measured level as a function of position for some frequencies of interest for fishing. The yellow line presents level reduction of $40log(r)$, which is expected when the Lloyd mirror effect is predominate. Figure 4.16 shows the measured noise spectrum in 1/3 octave band. The amplitude is 130 dB at $Freq = 80Hz$

Figure 4.15 and 4.16 implicated that the fish is capable of hearing the vessel at a distance of 500 m, Follow this trend that the fish can sense the vessel at a distance of 1000 m when the noise is at low frequency.

Section 2.3.2 mentioned that the noise generated by propeller cavitation which
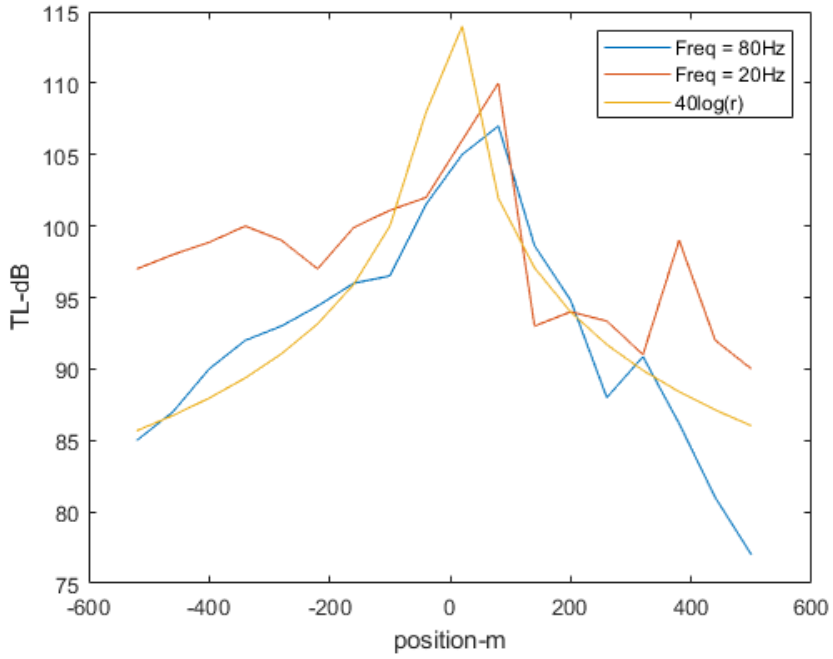
Figure 4.15: The transmission loss as a function of range and frequency

has peak power near 50-150 Hz, therefore the 80 Hz peak in the noise spectrum is caused by the propeller cavitation.
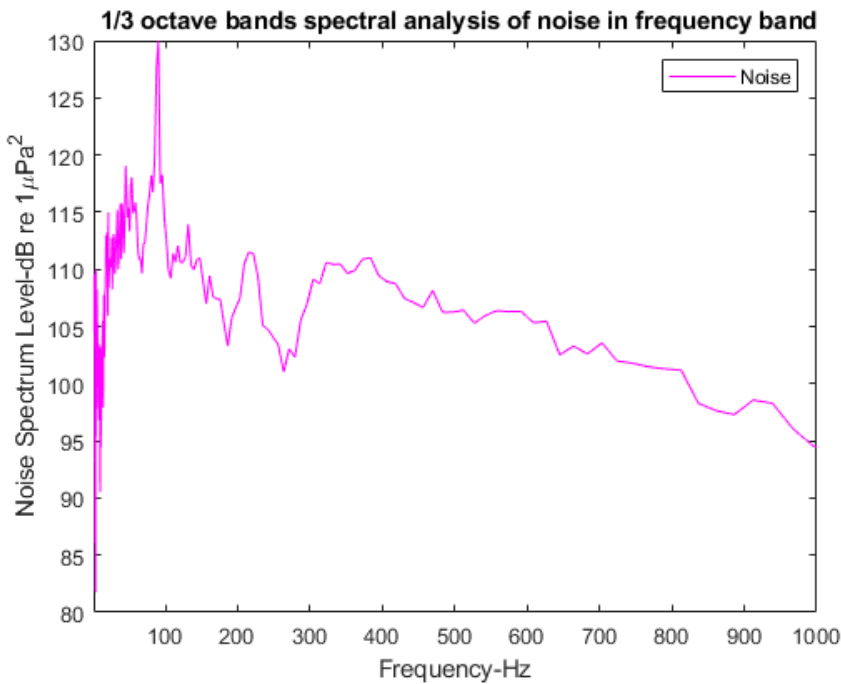
Figure 4.16: Noise spectrum in 1/3 octave bands

4.6 Time Difference Verses Range

Figure 4.17 presents the time differences between the direct and surface reflected increases as the distances between the vessel and sound source decreases. The furthest location has the smallest time difference since the source and image source can be considered as one source when the receiver located very very far from them (Distance $r >> wavelength$).
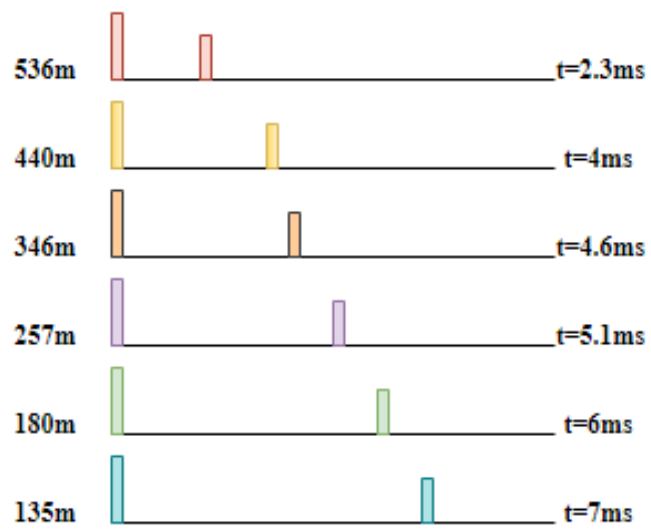
Figure 4.17: Time differences verses the range

Chapter 5

Conclusion

This thesis presented the design steps of a model, the model is used to compensate the Lloyd mirror effect thereby give a correction to the underwater noise level measurement.

The context was shown the Lloyd mirror effect caused maxima and minima in the noise intensity level. The comparison of the measured noise spectrum and Lloyd mirror effect corrected noise spectrum level showed that the simple inverse filter did correct the Lloyd mirror effect. The corrected noise spectrum was not as expected is may because the position of the hydrophones, not close enough to the sea bottom caused sea bottom reflection interference. The bottom reflection interference also caused maxima and minima in the noise intensity level. Underwater ambient noise and other ship noise also played a role here.

The vessel used to conduct the experiment is a research vessel not a fishing vessel with trawl. So the noise spectrum of trawling was still unknown. The noise spectrum of the research vessel shown peak at $Freq = 80Hz$, compared it to the commercial ship noise characteristics that this unpleasant noise was from propeller cavitation.

Appendix

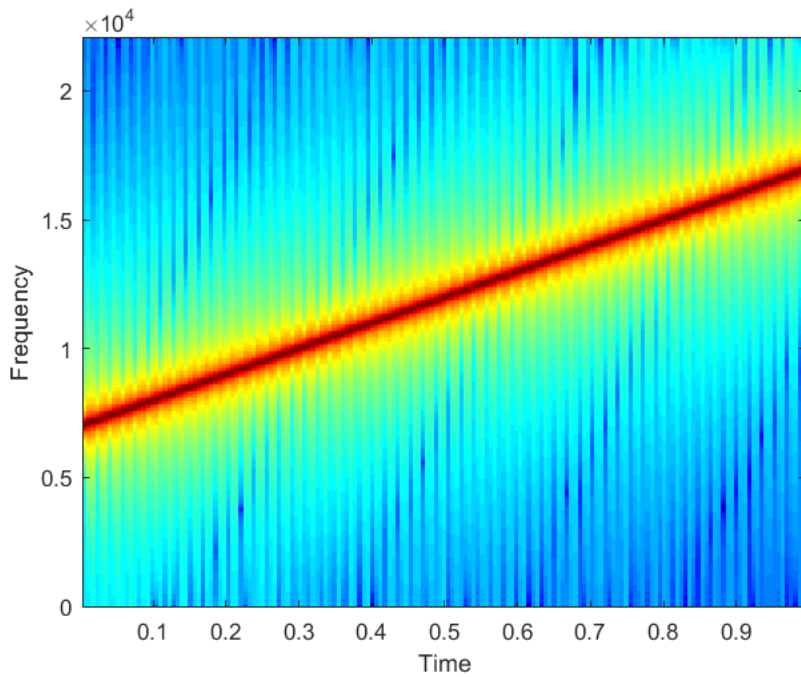## The chirp signal spectrum

Figure 5.1: Spectrum of chirp signal

Whole Range Channel Impulse Response

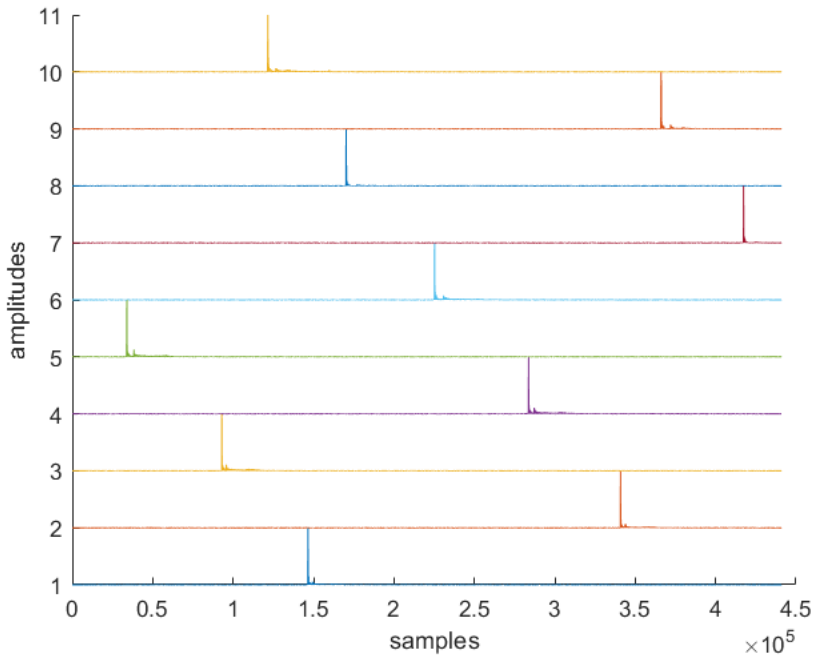
Figure 5.2: Channel impulse response

Bibliography

[1] Jens M Hovem *Marine Acoustics The physics of Sound in Underwater Environments*

[2] Urick RJ. 1983 . *Principles of underwater sound* Los Altos, CA : Peninsula Publishing . 423 pp.

[3] Wenz GM. 1962 . *Acoustic ambient noise in the ocean : spectra and sources* J. Acoust. Soc. Am. 34 : 1936 – 1956 .

[4] NRC . 2003 . *Ocean noise and marine mammals.* Washington, DC : National Research Council . 204 pp.

[5] Ross D. 1976. *Mechanics of underwater noise.* Oxford: Pergamon Press.

[6] Hildebrand JA.2009. Anthropogenic and natural sources of ambient noise in the ocean.*Marine Ecology Progress Series 395:5–20*

[7] McKenna MF, Wiggins SM, Hildebrand JA. 2013. . Relationship between container ship underwater noise levels and ship design, operational and oceanographic conditions.*Scientific Reports 3: Article 1760*

[8] Bassett C, Polagye B, Holt M, Thomson J. 2012. A vessel noise budget for Admiralty Inlet, Puget Sound, Washington (USA).*The Journal of the Acoustical Society of America* 132(6):3706-3719

[9] McKenna MF, Ross D, Wiggins SM, Hildebrand JA. 2012. Underwater radiated noise from modern commercial ships.*The Journal of the Acoustical Society of America* 131(1):92–103.

[10] Kipple B. 2002. Southeast Alaska cruise ship underwater acoustic noise. Technical Report NSWCCD-71-TR-2002/574, Naval Surface Warfare Center – Detachment Bremerton. *Available at* http://www.nps.gov/ glba/ nature-science/ upload/ CruiseShipSoundSignaturesSEAFAC.pdf

[11] Arveson PT, Vendittis DJ. 2000. Radiated noise characteristics of a modern cargo ship. *The Journal of the Acoustical Society of America* 107(1):118-129.

[12] WIKIPEDIA *Matched filter* `https://en.wikipedia.org/wiki/Matched-filter`

[13] T.C.Yang *Differences Between Passive-Phase Conjugation and Decision-Feedback Equalizer for Underwater Acoustic Communications*

[14] Jens M Hovem *Ray Trace Modeling of Underwater Sound Propagation*

[15] Mathias Fink *Time-reversed acoustics al 2000 Rep. Prog. Phys. 63 1933*

[16] Jens M Hove. 2018. *Undervanns støymåling med adaptive kanalutjevning*

[17] DNV. Dnv ship rules D2.5- Full Scale Radiated Noise Measurement Technical report, Det Norske Veritas, January 2010.

[18] Fujieda S, Matsuno Y and Yamanaka Y . 1996 .A *The auditory threshold of the bastard halibut Paralichthys olivaceus.* Nippon Suisan Gakkaishi . 62 : 201 − 204

[19] Popper AN and Fay RR . 1999 . *The auditory periphery in shes . In: Fay RR and Popper AN (eds). Comparative Hearing: Fish and Amphibians* . p:43 − 100 . New York : Springer - Verlag

[20] Mitson RB . 1993 . *Underwater noise radiated by research vessels* . ICES Mar. Sci. Symp. 196 : 147 − 152 .

[21] Popper AN . 2003 . *Effects of anthropogenic sounds on fishes.* Fisheries 28 (10): 24 − 31 .